



**HAL**  
open science

## Accessing quantitative degrees of functionalization on solid substrates via solid-state NMR spectroscopy

Marianne Gaborieau, Leena Nebhani, Robert Graf, Leonie Barner,  
Christopher Barner-Kowollik

► **To cite this version:**

Marianne Gaborieau, Leena Nebhani, Robert Graf, Leonie Barner, Christopher Barner-Kowollik. Accessing quantitative degrees of functionalization on solid substrates via solid-state NMR spectroscopy. *Macromolecules*, 2010, 43 (8), pp.3868 - 3875. 10.1021/ma100149p . hal-04082621

**HAL Id: hal-04082621**

**<https://hal.science/hal-04082621v1>**

Submitted on 26 Apr 2023

**HAL** is a multi-disciplinary open access archive for the deposit and dissemination of scientific research documents, whether they are published or not. The documents may come from teaching and research institutions in France or abroad, or from public or private research centers.

L'archive ouverte pluridisciplinaire **HAL**, est destinée au dépôt et à la diffusion de documents scientifiques de niveau recherche, publiés ou non, émanant des établissements d'enseignement et de recherche français ou étrangers, des laboratoires publics ou privés.

# Accessing Quantitative Degrees of Functionalization on Solid Substrates via Solid State NMR Spectroscopy

*Marianne Gaborieau<sup>1\*</sup>, Leena Nebhani<sup>2</sup>, Robert Graf<sup>1</sup>, Leonie Barner<sup>3\*</sup> and  
Christopher Barner-Kowollik<sup>2\*</sup>*

<sup>1</sup>Max Planck Institute for Polymer Research, Ackermannweg 10, 55128 Mainz, Germany,  
[m.gaborieau@uws.edu.au](mailto:m.gaborieau@uws.edu.au), [graf@mpip-mainz.mpg.de](mailto:graf@mpip-mainz.mpg.de)

<sup>2</sup>Preparative Macromolecular Chemistry, Institut für Technische Chemie und Polymerchemie,  
Karlsruhe Institute of Technologie (KIT), Engesserstrasse 18, 76128 Karlsruhe, Germany,  
[leena.nebhani@kit.edu](mailto:leena.nebhani@kit.edu), [christopher.barner-kowollik@kit.edu](mailto:christopher.barner-kowollik@kit.edu)

<sup>3</sup>Fraunhofer Institut für Chemische Technologie, Joseph-von-Fraunhofer-Strasse 7, 76327 Pfinztal  
(Berghausen), Germany, [leonie.barner@ict.fraunhofer.de](mailto:leonie.barner@ict.fraunhofer.de).

## RECEIVED DATE

**TITLE RUNNING HEAD:** Solid-state NMR microsphere functionalization

**CORRESPONDING AUTHORS:** [m.gaborieau@uws.edu.au](mailto:m.gaborieau@uws.edu.au), +61 2 4620 3060, +61 2 4620 3025;  
[leonie.barner@ict.fraunhofer.de](mailto:leonie.barner@ict.fraunhofer.de), +49 721 4640 872, +49 721 4640 111; [christopher.barner-kowollik@kit.edu](mailto:christopher.barner-kowollik@kit.edu), +49 721 608 5641, +49 721 608 5740. M. Gaborieau has moved to the Nanoscale and Dynamics Organization group, University of Western Sydney, Campbelltown Campus, Building 21, Locked Bag 1797, Penrith South DC NSW 1797, Australia.

**ABSTRACT** The development of a solid-state nuclear magnetic resonance (NMR) method allowing the quantification of active sites (i.e. residual vinyl groups) accessible for chemical functionalization

on the surface of poly(divinyl benzene) microspheres is presented. Residual vinyl groups of poly(divinyl benzene) microspheres (PDVB55 and PDVB80) were quantified via solid-state  $^{13}\text{C}$  Cross-Polarization Magic Angle Spinning (CP-MAS) NMR spectroscopy. In addition,  $^{13}\text{C}$  CP-MAS NMR spectroscopy allows the comparison of core and grafted microspheres functionalization on the same (arbitrary) scale in a short measuring time. This scale was calibrated by an extended absolute quantification of the vinyl groups using  $^{13}\text{C}$  single pulse excitation (SPE) MAS NMR spectroscopy. The degree of crosslinking of the microspheres was calculated to be 30% and 50% for PDVB55 and PDVB80 microspheres, respectively. The number of active groups per nominal surface area is 110 and 179 groups per  $\text{nm}^2$  for PDVB55 and PDVB80 microspheres, respectively. The loading capacities of the microspheres (e.g. 0.61 and 0.65  $\text{mmol}\cdot\text{g}^{-1}$ ) are similar to ones found in Merrifield resins of comparable sizes.

**KEYWORDS:** Surface Functionalization; Quantitative Surface Analysis; Microspheres; Solid State Nuclear Magnetic Resonance Spectroscopy.

## Introduction

Functional polymeric microspheres have a high potential in medical and biomedical applications, such as drug delivery systems, in medical diagnostics or as contrast agents for X-ray imaging, as stationary phases for chromatography or for the detection of degradation products of chemical weapons.<sup>1, 2</sup> Polymeric microspheres can be synthesized directly by heterogeneous polymerization techniques, e.g. emulsion and dispersion polymerization.<sup>2</sup> In addition, highly crosslinked mono- and narrow-disperse poly(divinyl benzene) microspheres can be synthesised via precipitation polymerization.<sup>3</sup> Microspheres synthesized via this technique are free of surfactants or stabilizers, instead they have residual vinyl groups on their surface. These residual vinyl groups open the possibility to graft a polymeric shell from or to an existing particle thus constituting an ideal synthetic handle for the preparation of core-shell microspheres and add further chemical functionalities to the particles. So far, a wide variety of

techniques have been used to functionalize these microspheres, including controlled/'living' radical polymerization,<sup>4-8</sup> anionic ring-opening polymerization,<sup>9</sup> and highly orthogonal 'click' chemistry.<sup>10-13</sup> In order to exploit the full potential of these functional microspheres, it is extremely valuable to have information about the amount of accessible active sites (e.g. vinyl groups) on the surface of the particles.<sup>1</sup> Being highly crosslinked, these systems are insoluble and must be characterized in the gel state or the solid state.

To the best of our knowledge, the only characterization of poly(divinyl benzene)-based microspheres in terms of residual vinyl groups was so far carried out qualitatively by infrared spectroscopy (IR).<sup>14</sup> IR spectroscopy detects the residual vinyl groups through resonances at 1 600 and 990 cm<sup>-1</sup>. Crosslinked polystyrene gels were characterized by high-resolution magic-angle spinning (HR-MAS) NMR spectroscopy.<sup>15-18</sup> Well-resolved <sup>1</sup>H and <sup>13</sup>C NMR spectra were obtained through efficient averaging of chain orientation along the axes between crosslinking points, allowing observing the chemical functionalization. However, it is unclear if the monomer units close to the crosslinking points are contributing to the observed signals due to their slower local dynamics.<sup>16, 17, 19</sup> Residual vinyl groups in poly(divinyl benzene)-based networks were analyzed by <sup>13</sup>C solid-state NMR spectroscopy and a wet chemical method, e.g. bromination. Noting that <sup>13</sup>C cross-polarization NMR is intrinsically not quantitative and that bromination is not quantitative because of side reactions and limited reagents accessibility to highly crosslinked regions, the authors concluded that no method is available yet for accurate, quantitative analysis of the residual vinyl groups.<sup>17</sup> In the current study, solid-state NMR spectroscopy was applied to polymer systems exhibiting homogeneous local mobility and homogeneous <sup>1</sup>H density, in which all sample parts contribute to the NMR signal without bias. The investigated microspheres are formed by distillation-precipitation polymerization, a process during which the polymer chains gradually precipitate onto the particles as they are polymerized; no stabilizer or further additives are used. Furthermore, their surface is (highly) porous, and they are best described as porous particles than as bulk particles limited by a sharp surface. We thus expect these pure poly(divinyl

benzene) particles with homogenous chain topology to exhibit homogeneous local mobility and  $^1\text{H}$  density across the whole sample in the solid state.

Solid-state NMR spectroscopy is a versatile technique for the characterization of local structure and dynamics in polymers.<sup>20-25</sup>  $^{13}\text{C}$  solid-state NMR spectroscopy under magic-angle spinning (MAS) exhibits significantly higher resolution than  $^1\text{H}$  solid-state NMR spectroscopy but lower sensitivity, because only 1% of the carbon nuclei are NMR-sensitive  $^{13}\text{C}$  nuclei. The sensitivity issue of the common  $^{13}\text{C}$  single-pulse excitation (SPE) NMR spectroscopy can be overcome by the use of cross-polarization (CP), which consists in transferring magnetization from  $^1\text{H}$  to  $^{13}\text{C}$  nuclei before recording  $^{13}\text{C}$  signals. CP takes advantage of the higher natural abundance and faster relaxation of  $^1\text{H}$  spins compared to  $^{13}\text{C}$  ones.<sup>26, 27</sup> It generally yields higher intensities, but is usually not quantitative because of different cross-polarization efficiencies and relaxation properties of the observed groups. Alternative pulse schemes have recently been proposed to record quantitative CP-MAS spectra.<sup>28-31</sup> Although these allow for more uniform CP dynamics, the measurements still suffer from adverse effects of the short relaxation properties or heterogeneous local mobility<sup>29</sup> or need extensive complementary measurements to correct the experimental CP intensity.<sup>31</sup> Lowering the temperature of the measurements may help reducing the local dynamic heterogeneity, but is experimentally more challenging.<sup>32</sup>

In the current study, we present the development of a solid-state nuclear magnetic resonance (NMR) method allowing – for the first time – the quantification of active sites (i.e. residual vinyl groups) accessible for chemical functionalization on the surface of poly(divinyl benzene) (PDVB) microspheres.

## Experimental Section

**Materials.** Technical-grade divinyl benzene (DVB55 containing 55 wt.-% divinyl benzene isomers, Aldrich and DVB80 containing 80 wt.-% divinyl benzene isomers, Aldrich), and *n*-butyl acrylate (99%, Fluka) was purified by percolation through a column of activated basic alumina. 2,2'-Azobisisobutyronitrile (AIBN) was purchased from Aldrich and recrystallized twice from ethanol. Cyanopropyl dithiobenzoate (CPDB) was synthesized according to the literature and its purity was

confirmed by NMR spectroscopy.<sup>33</sup> Acetonitrile, dichloromethane, tetrahydrofuran, toluene, ethanol, methanol and acetone were all used as received.

**Synthesis of PDVB80 and PDVB55 Microspheres via Distillation-Precipitation Polymerization.**

PDVB80 and PDVB55 microspheres were synthesized by distillation-precipitation polymerization.<sup>34</sup> AIBN (0.092 g, 0.56 mmol, 2 wt.-% relative to the total monomer) and DVB80 or DVB55 (5 mL, 4.6 g, 35.35 mmol, 2.5 vol.-% relative to the reaction medium) was dissolved in 200 mL of acetonitrile in a 500 mL round-bottom flask, attached to a distillation assembly. The reaction mixture was heated from ambient temperature to boiling state by ramping the temperature gradually, until the solvent started distilling. As the solvent started distilling the initially homogenous reaction mixture turned milky white. The reaction was stopped after half of the initial acetonitrile used in reaction mixture was collected in the receiving flask. After the polymerization was finished, the resulting PBVB80 or PDVB55 microspheres were separated by filtration through a 0.45  $\mu\text{m}$  membrane, washed and re-suspended several times in toluene, THF, acetone and diethylether. The washing of the microspheres with toluene is very critical in this case as through washing with toluene it is possible to remove the residual monomer (see below). The microspheres were dried in a vacuum oven at 40 °C before characterization. 1.36 g of PDVB80 and 1.5 g of PDVB55 were obtained in 30% and 33% yield respectively.

**Synthesis of Hydroxy Functionalized PDVB80 and PDVB55 Microspheres.** PDVB80 or PDVB55 microspheres (1.0 g) were suspended in dry THF (10 mL) in a dry 100 mL round-bottom flask for 2 h, and 0.1 g (2.6 mmol) of sodium borohydride was added. The suspension was cooled in a cold-water bath, and 0.376 g (2.6 mmol) of boron trifluoride diethyl etherate dissolved in 1 mL of THF was added dropwise to the suspension of microspheres. The temperature of the reaction suspension was maintained at 20 °C during the addition of  $\text{BF}_3$  and further for 3 h. At the end of this period, the flask was immersed in an ice bath, and 5 mL of cold water was slowly added to destroy any residual  $\text{NaBH}_4$ . Subsequently, hydrogen peroxide (0.8 mL, 30% in water, 36 mmol) was slowly added to the reaction mixture. During the addition, the pH of the solution was maintained near  $\text{pH} = 8$  by adding  $3 \text{ mol} \cdot \text{L}^{-1}$  sodium hydroxide as needed. The final solution was filtered through a 0.45  $\mu\text{m}$  membrane filter and washed with water

(pH = 8) followed by methanol. The resulting microspheres were dried in a vacuum oven before characterization.

**Grafting of *n*-Butyl Acrylate from Microspheres.** All RAFT polymerizations were carried out in toluene. A solution of *n*-butyl acrylate (19.45 g), AIBN (0.0318 g,  $3.7 \cdot 10^{-3} \text{ mol} \cdot \text{L}^{-1}$ ) and CPDB (0.15 g,  $1.2 \cdot 10^{-2} \text{ mol} \cdot \text{L}^{-1}$ ) in toluene (35 mL) was prepared. 5 mL of the above solution was transferred into glass sample vials, each containing 300 mg of the microspheres. The sample vials were capped with rubber septa and deoxygenated by purging with nitrogen for 15 min. The samples were stirred with a magnetic bar at 80 °C. The polymerization was stopped after 3 h. The resulting grafted microspheres were isolated by filtration through a 0.45  $\mu\text{m}$  membrane, washed several times with toluene and dichloromethane and dried in a vacuum oven overnight. Polymers from the solutions were collected to determine the molecular weight by SEC ( $M_n = 18\,000 \text{ g} \cdot \text{mol}^{-1}$ ,  $D_M = 1.2$  for PDVB80 and  $M_n = 19\,000 \text{ g} \cdot \text{mol}^{-1}$ ,  $D_M = 1.2$  for PDVB55).

**Routine characterization.** The morphology of the microspheres was established with a Hitachi S900 scanning electron microscope (SEM). The microspheres were dispersed in ethanol; a drop of this particle suspension was cast onto an electron microscope stub covered with a double-sided carbon tape which in turn is covered with a 5 mm glass cover slip. Samples were sputter-coated with chromium. Electron micrographs of each sample were recorded at different magnifications. The particle size analysis from SEM micrograph was done for an average of 100 microspheres.  $D_n$ ,  $D_w$  and  $U$  were calculated using the following equations:  $D_n = \sum n_i D_i / \sum n_i$ ,  $D_w = \sum n_i D_i^4 / \sum n_i D_i^3$ ,  $U = D_n / D_w$ , where,  $D_n$  is the number average diameter,  $D_w$  is the weight average diameter, and  $U$  is the polydispersity index. The  $D_n$ ,  $D_w$  and  $U$  for PDVB80 microspheres is 1.51  $\mu\text{m}$ , 1.51  $\mu\text{m}$  and 1.00 respectively. The  $D_n$ ,  $D_w$  and  $U$  for PDVB55 microspheres is 1.59  $\mu\text{m}$ , 1.62  $\mu\text{m}$  and 1.01 respectively.

SEC measurements were performed on a Polymer Laboratories PL-GPC 50 Plus Integrated System, comprising an auto injector, a PLgel 5  $\mu\text{m}$  bead-size guard column (50  $\cdot$  7.5 mm), followed by three PLgel 5  $\mu\text{m}$  MixedC columns (300  $\cdot$  7.5 mm), and a differential refractive index detector using THF as the eluent at 35 °C with a flow rate of 1 mL  $\cdot$  min<sup>-1</sup>. The SEC system was calibrated using 6

polystyrene standards ranging from 160 to  $6 \cdot 10^6$  g·mol<sup>-1</sup> and linear poly(methyl methacrylate) standards ranging from 700 to  $2 \cdot 10^6$  g·mol<sup>-1</sup>. The resulting molecular weight distribution has been corrected using the Mark-Houwink relationship with  $K = 12.8 \cdot 10^{-5}$  dL · g<sup>-1</sup>,  $\alpha = 0.69$  for poly(methyl methacrylate),  $K = 14.1 \cdot 10^{-5}$  dL · g<sup>-1</sup>,  $\alpha = 0.7$  for polystyrene and  $K = 12.2 \cdot 10^{-5}$  dL · g<sup>-1</sup>,  $\alpha = 0.70$  for poly(*n*-butyl acrylate).<sup>23, 35, 36</sup> An alternative SEC data treatment taking into account the possible influence of long-chain branching<sup>24, 37-39</sup> was outside the scope of the present study. The structure of the synthesized RAFT agent (CPDB) was confirmed by <sup>1</sup>H and <sup>13</sup>C solution-state NMR spectroscopy using a Bruker AM 400 spectrometer at Larmor frequencies of 400 MHz for <sup>1</sup>H nuclei and 100 MHz for <sup>13</sup>C nuclei. All samples were dissolved in CDCl<sub>3</sub>. The chemical shift scale is internally referenced to tetramethylsilane at 0.00 ppm.

The density of the PDVB microspheres in ethanol was determined using a density meter (DMA 5000 M, Anton Paar) at 293K. The particle density was found to be 1.82 g·cm<sup>-3</sup> and 1.12 g·cm<sup>-3</sup> for PDVB80 and PDVB55 microspheres, respectively.

**Solid-state NMR spectroscopy.** <sup>1</sup>H MAS NMR spectroscopy was carried out on a Bruker Avance spectrometer (Bruker BioSpin, Germany) operating at a <sup>1</sup>H Larmor frequency of 700.13 MHz using a 2.5 mm solid-state MAS NMR probehead and a MAS rotational frequency of 30 kHz. Spectra were recorded using a 2.5 μs 90° pulse, 16 transients and 5 s repetition delay.

<sup>13</sup>C SPE-MAS NMR was carried out on a Bruker Avance spectrometer (Bruker BioSpin, Germany) operating at a <sup>13</sup>C Larmor frequency of 175 MHz using a 4 mm solid-state MAS NMR probehead and a MAS rotational frequency of 18 kHz. Spectra were recorded using a 4 μs 90° pulse, 7062 transients (8064 transients for background) and 60 s repetition delay.

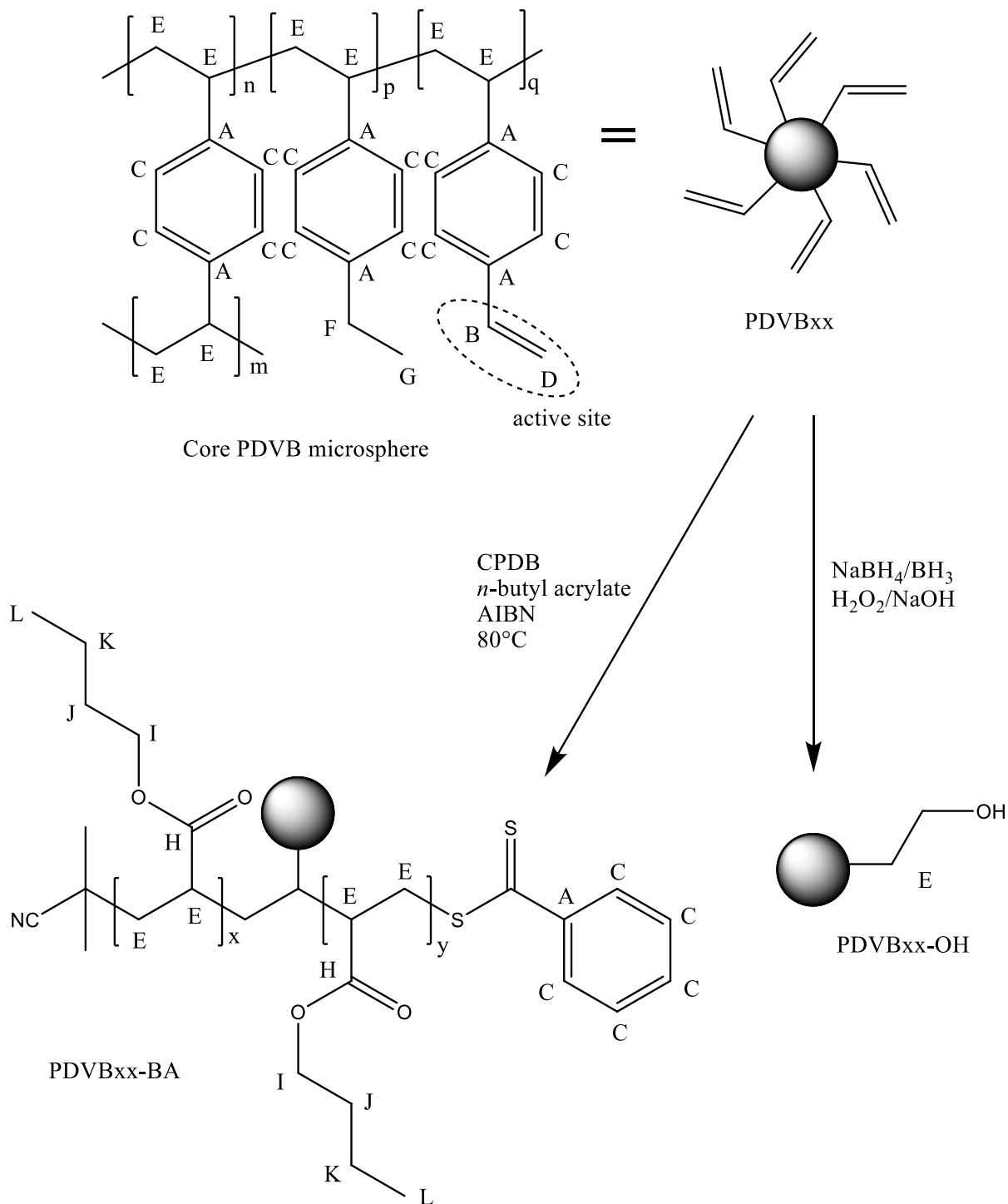
<sup>13</sup>C CP-MAS NMR spectroscopy was carried out on a Bruker Avance spectrometer (Bruker BioSpin, Germany) operating at a <sup>13</sup>C Larmor frequency of 125.75 MHz using a 2.5 mm solid-state MAS NMR probehead and a MAS rotational frequency of 18 kHz. Spectra were recorded using a 2.5 μs 90° pulse, 2 ms contact time, 5 632 transients (1 024 transients for sample PDVB55 with variable contact time)



and 5 s repetition delay. A detailed signal assignment<sup>17, 18, 40, 41</sup> is given in the Supporting Information section. Signals C and D were integrated over the ranges from 134 to 118 ppm and from 118 to 107.5 ppm, respectively.

## Results and Discussion

The highly cross-linked PDVB microspheres employed in the current work were synthesized by distillation-precipitation polymerization. This technique only requires divinyl benzene (DVB) (which is also a cross-linker), a radical initiator, 2,2'-azoisobutyronitrile (AIBN), and a near  $\Theta$ -solvent for DVB (acetonitrile). DVB is available in two technical grades, DVB55 and DVB80, which are composed of isomers of DVB and 3- and 4-ethylvinyl benzene. 3- and 4-ethylvinyl benzene have only one functional vinyl group and can for this reason not act as a cross-linker. Core microspheres therefore exhibit three types of structural aromatic units in the backbone of PDVB as depicted on the upper left hand side in Scheme 1 (note that isomeric structures are not included). One structure is based on a DVB unit where both vinyl groups have reacted; forming the cross-linked network, in the other case only one of the two vinyl groups has reacted, resulting in a residual vinyl group. In addition, a further structural entity results from the incorporated 3- or 4-ethylvinyl benzene. This structural entity therefore does not include a residual vinyl group, but an ethyl group. In the subsequent modification of the microspheres only the residual vinyl groups (also termed 'active' sites) are involved in the 'grafting from' polymerization and therefore a simplified representation of the core microspheres including only these active sites is depicted on the upper right side of Scheme 1. The capital letters next to the atoms in Scheme 1 are used for the complete chemical shift assignments in the <sup>13</sup>C NMR spectra (refer to the Supporting Information section, Table S1).



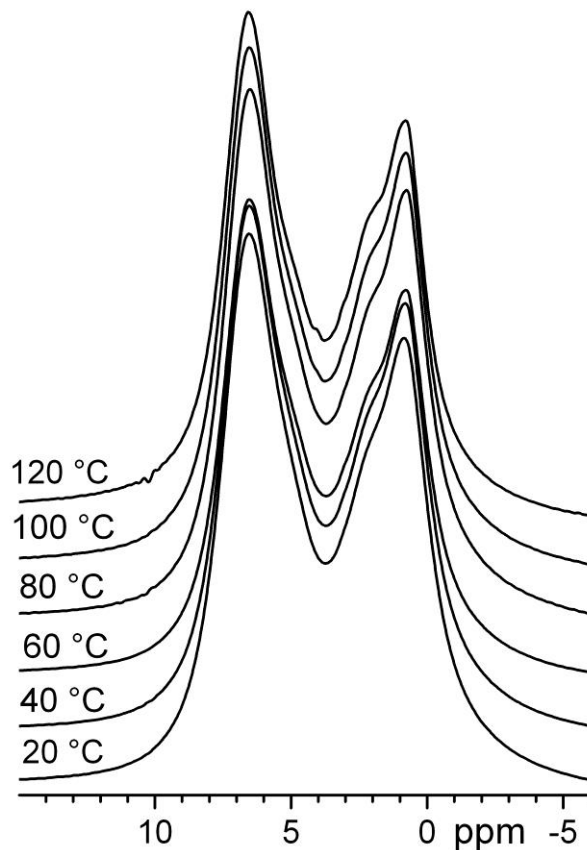
**Scheme 1.** Schematic representation of the core, hydroxylated and poly(*n*-butyl acrylate)-graft-poly(divinyl benzene) microspheres. Capital letters relate to the <sup>13</sup>C chemical shift assignment in Figure 2.

Residual vinyl groups, e.g. ‘active’ sites, are present within and on the surface of the particle. However, residual vinyl groups in the centre of the particle are not easily accessible for reagents (e.g. reagents cannot easily diffuse to the centre of the microspheres due to the highly crosslinked nature of the particles), therefore not all of the ‘active’ sites will be able to take part in the subsequent modification of the particles via ‘grafting from’ polymerization. Only a certain degree of the ‘active’ sites will be accessible for further functionalization. In order to estimate the number of ‘accessible active’ sites, the residual vinyl groups of the PDVB microspheres which are accessible for reagents were hydroxylated (see Scheme 1, lower right side).

In addition, core PDVB microspheres were functionalized by grafting *n*-butyl acrylate (BA) from the microspheres using the RAFT agent cyanopropyl dithiobenzoate (CPDB), resulting in PDVB-*g*-PBA-microspheres (see Scheme 1, lower left side). Subsequently, all synthesized microspheres were characterized via <sup>1</sup>H and <sup>13</sup>C NMR spectroscopy to quantitatively assess the degrees of functionalization.

<sup>1</sup>H solid-state NMR spectra recorded at high field under fast MAS showed insufficient resolution for selectively observing signals from vinyl groups, expected in the 6 to 7 ppm range (Figure 1). The only resolved signals are indeed a massif of aliphatic signals, centered around 1 ppm, and a massif of aromatic and unsaturated signals centered around 6 ppm. Signals may be broad because of the low mobility of the samples due to their high degree of crosslinking. No significant change in the spectrum of PDVB55 was observed upon heating up to 120 °C (Figure 1). Therefore <sup>1</sup>H solid-state NMR spectroscopy is not appropriate for observing or quantifying active sites in PDVB microspheres, because of its limited resolution. Note that weak narrow signals were originally observed at 5.2, 6.2 and 6.7 ppm for the sample PDVB80 (see Supporting Information, Figure S1), which originate from vinyl groups.<sup>5</sup> These signals disappeared upon repeated washing of the sample with toluene and were thus assigned to residual monomer units rather than active sites (residual vinyl groups on the polymer chains). Care was taken to ensure that all core PDVB microspheres used for the present work had been washed

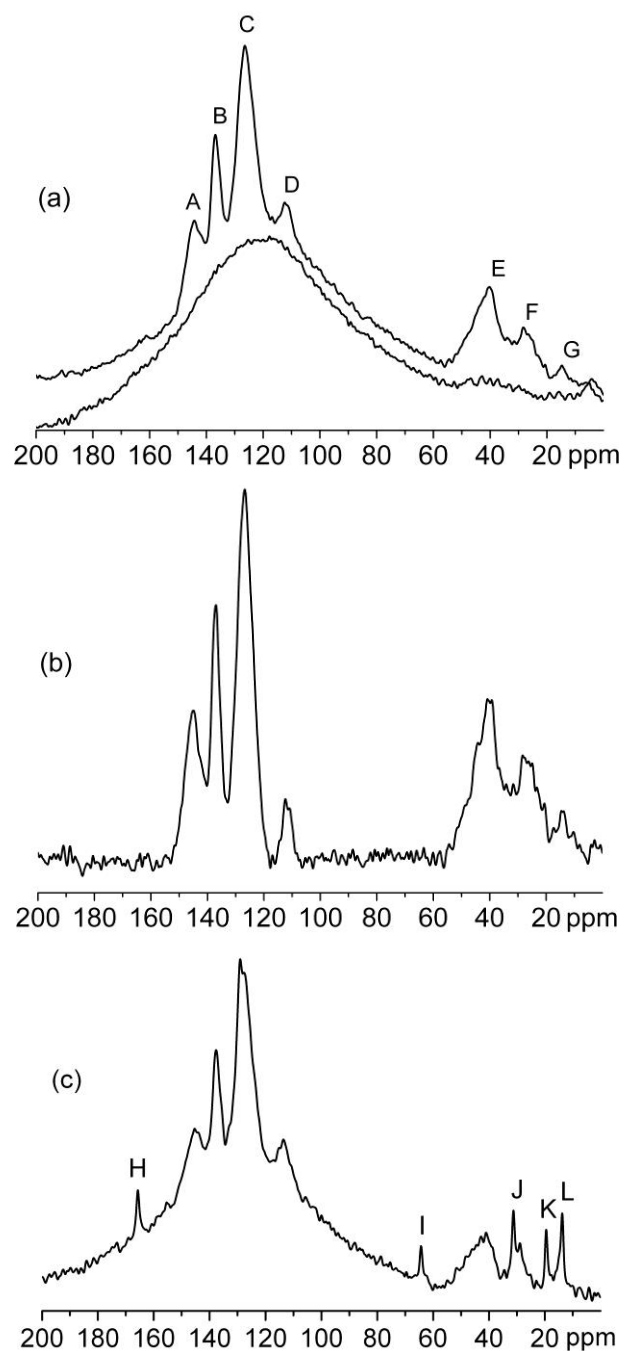
appropriately to remove any residual monomer, before functionalization or NMR measurement. Careful purification is particularly important since the signal of vinyl groups from residual monomer would overlap with those from the polymer chains, inducing an error in the active sites quantified by  $^{13}\text{C}$  NMR spectroscopy.



**Figure 1.**  $^1\text{H}$  solid-state NMR spectra at high field and fast MAS of PDVB55 microspheres at different temperatures.

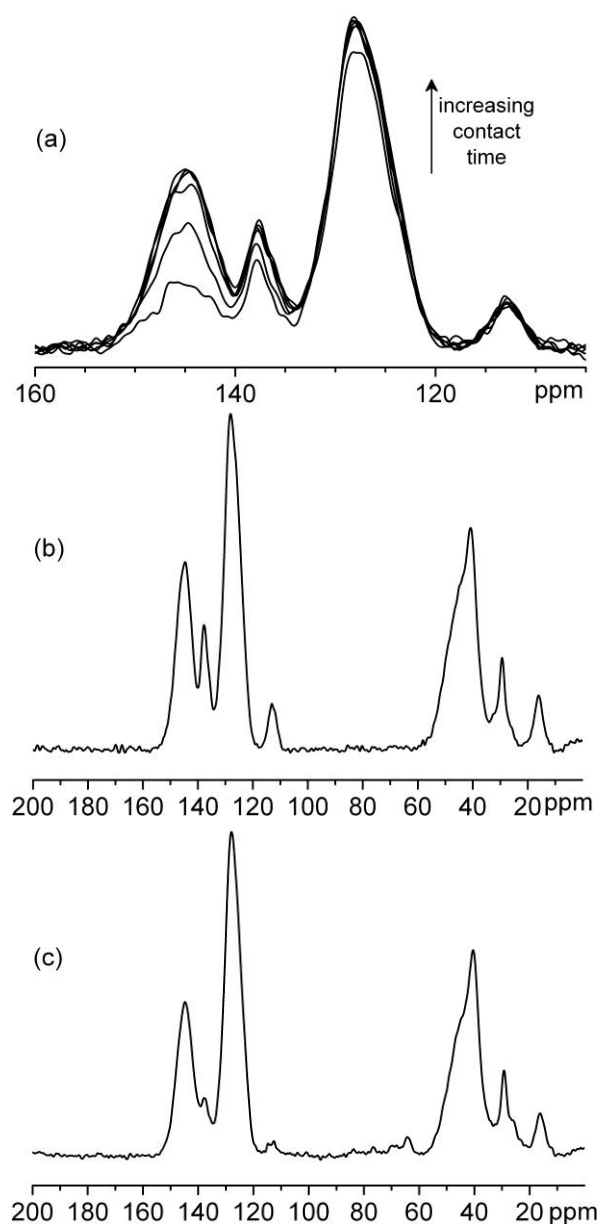
Improved resolution was sought through  $^{13}\text{C}$  solid-state NMR spectroscopy.  $^{13}\text{C}$  SPE-MAS NMR spectroscopy allows the observation of a resolved signal at 113 ppm for the active site. It originates in the methylene carbon of the vinyl groups pending from the polymer chain (signal D on Figure 2a for PDVB80, see Scheme 1 and Supporting Information Table S1 for complete signals assignment). The signal at 128 ppm (C on Figure 2a) solely originates in the non-substituted carbons of the aromatic rings (4 per monomer units). In terms of chemical shift and shape of signal observed in  $^{13}\text{C}$  SPE-MAS spectra, sample PDVB80 (Figure 2a) is representative of core and hydroxylated microspheres,

while sample PDVB80-BA (Figure 2c) is representative of poly(*n*-butyl acrylate)-grafted microspheres. The active sites can in principle be quantified in percents of the monomer units by  $^{13}\text{C}$  NMR spectroscopy via signals D and C for all samples. However, a broad signal underlying the aromatic region was observed with an intensity comparable to that of the signals of interest. The broad underlying signal renders the quantification of the narrow C and D signals difficult. Possible causes for the observation of the broad signal were subsequently examined. Signal broadening due to paramagnetic impurities was ruled out since no paramagnetic species were present in any step of the synthesis. The broad signal may originate in highly-crosslinked samples parts, which would be locally less mobile than the rest of the sample. If this was the case, the signal should narrow with increasing local mobility upon heating. Variable-temperature experiments showed that this was not the case (see the Supporting Information section for details, Figure S2). Thus the broad underlying signal most probably originates from components other than the sample, namely the cap of the rotor containing the sample and various components of the probe. This was checked by comparing the  $^{13}\text{C}$  SPE-MAS spectra of sample PDVB80 in a given rotor and of the same empty rotor under the exact same conditions (Figure 2a): the broad underlying signal observed for PDVB80 exactly overlays with the background signal. Thus the quantification of signals C and D is possible on a quantitative  $^{13}\text{C}$  SPE-MAS spectrum after subtraction of the background signals. The acquisition of a quantitative spectrum however was found to require prohibitively long measuring times to be carried out on all samples (see below).



**Figure 2.**  $^{13}\text{C}$  solid-state SPE-MAS NMR spectra of (a, top) PDVB80 microspheres, (a, bottom) background, and (c) PDVB80-BA microspheres, (b) shows the subtraction of the spectra of PDVB80 microspheres and background (a). The letters refer to Scheme 1; a complete  $^{13}\text{C}$  chemical shift assignment is given in Supporting Information, Table S1.

Improved sensitivity was therefore sought through  $^{13}\text{C}$  CP-MAS NMR spectroscopy. It overcame two problems: spectra with a resolved signal from the methylene group of the active site at 113 ppm could be recorded in shorter times without background signal (Figure 3b).  $^{13}\text{C}$  CP-MAS spectra are not intrinsically quantitative. However, a range of contact times was identified, over which the relative intensities of the signals of interest did not vary, allowing quantitative comparison between samples on the same arbitrary scale (Figure 3a). The representative  $^{13}\text{C}$  CP-MAS spectra of PDVB55 and PDVB55-BA are shown in Figure 3b and 3c, spectra are shown for other samples in the Supporting Information in Figure S3.



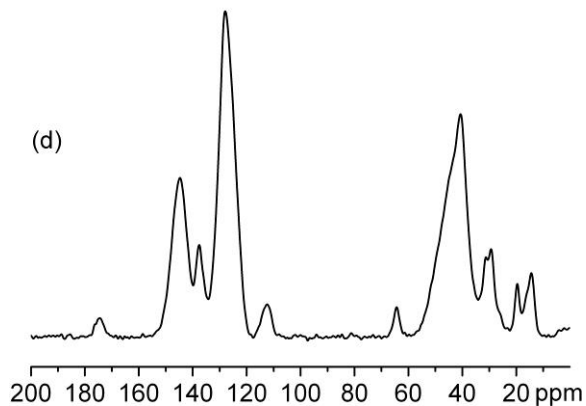


**Figure 3.**  $^{13}\text{C}$  solid-state CP-MAS NMR spectra of (a) PDVB55 microspheres with short measuring time and variable contact time (250  $\mu\text{s}$ , 500  $\mu\text{s}$ , 1 ms, 2 ms, 2.5 ms, 3 ms), (b) PDVB55, (c) PDVB55-OH and (d) PDVB55-BA microspheres.

The active sites  $AS$  (i.e. residual vinyl groups on the polymer chains) were quantified from  $^{13}\text{C}$  CP-MAS spectra, on the same arbitrary scale with respect to the monomer units, using equation (1):

$$AS \text{ (a.u.)} = \frac{100 \cdot I(D) \cdot 4}{I(C)} \quad (1)$$

where  $I(D)$  is the area of the signal centered around 113 ppm, originating solely in one (methylene) carbon of residual vinyl groups, and  $I(C)$  is the area of the signal centered around 128 ppm, originating solely in four carbons per phenyl group of the monomer unit (unsubstituted carbons). Active sites quantified on the same arbitrary scale are given for all samples in Table 1. The peak at 128 ppm is not fully resolved from the signals centered around 138 and 145 ppm; however, considering the similar signal areas present on both sides of the minimum at 134 ppm, the error introduced is small compared to the experimental error, and systematic for all samples. Note that for the samples grafted with poly(*n*-butyl acrylate), the signal centered around 128 ppm also contains the signal of the 5 non-substituted aromatic carbons of the RAFT group, which is assumed to be negligible compared to the experimental error made during the measurements. Such an assumption is supported by the fact that the C=S signal of the same RAFT group at approximately 225 ppm is below the detection limit for both PDVB55-BA and PDVB80-BA microspheres (see Supporting Information, Figure S4). Solid-state NMR 15



spectroscopy measures the whole sample volume and not only its surface; therefore the active sites are quantified throughout the sample. Active sites inside the microspheres, however, will not be accessible for functionalization because reagents will not be able to penetrate the microspheres to react with them. Active sites accessible for functionalization (*ASAF*) may however be quantified via comparison of active sites remaining after hydroxylation  $AS_{\text{hydroxylated}}$  with the active sites present in the corresponding core microspheres  $AS_{\text{core}}$ , using equation (2):

$$ASAF (\%) = \frac{100 \cdot (AS_{\text{core}} - AS_{\text{hydroxylated}})}{AS_{\text{core}}} \quad (2)$$

Similarly, an absolute quantification of the active sites actually functionalized during PBA-grafting, in percent of the active sites originally present on the core microspheres, may be calculated by replacing  $AS_{\text{hydroxylated}}$  by  $AS_{\text{PBA-grafted}}$  in Equation (2). *ASAF* values are shown for all hydroxylated and PBA-grafted samples in Table 1.

Residual vinyl groups are quantified with Equation (1) on the same arbitrary scale. This scale can be calibrated with the measurement of *AS* in percents of the monomer unit of one sample in a quantitative way. A quantitative  $^{13}\text{C}$  SPE-MAS spectrum can be recorded using a sufficiently long relaxation delay between scans to ensure full sample relaxation. Comparison of the spectra of PDVB80 recorded with relaxation delays ranging from 2 to 20 s indicated that a relaxation delay of 10 s is not sufficient to ensure full relaxation (see Supporting Information, Figure S5). Therefore a very long relaxation delay of 60 s was chosen. To increase the sensitivity, a larger sample volume was measured (filling a 4 mm rotor rather than a 2.5 mm rotor). A quantitative  $^{13}\text{C}$  SPE-MAS spectrum of PDVB80 was recorded, using a sufficiently long relaxation delay between scans to ensure full sample relaxation (Figure 2a). A  $^{13}\text{C}$  SPE-MAS spectrum of the empty rotor was subsequently recorded under the exact same experimental conditions to yield the background signal (Figure 2a). The subtraction of the background from the  $^{13}\text{C}$  SPE-MAS spectrum of sample PDVB80 yields the quantitative  $^{13}\text{C}$  SPE-MAS spectrum of sample PDVB80 (Figure 2b).

**Table 1.** Overview of the quantitative degrees of functionalization for various microspheres as described in Scheme 1.

Sample	<i>AS</i> (a.u.) <sup>a</sup>	<i>ASAF</i> (%) <sup>b</sup>	<i>AS</i> (%) <sup>c</sup>	<i>CL</i> (%) <sup>d</sup>	<i>F</i> <sub>mon</sub> (%) <sup>e</sup>	<i>F</i> <sub>part</sub> (groups particle <sup>-1</sup> ) <sup>f</sup>	<i>F</i> <sub>surf</sub> (groups nm <sup>-2</sup> ) <sup>g</sup>	<i>LC</i> (mmol g <sup>-1</sup> ) <sup>h</sup>
PDVB55-1	29		22	33				
PDVB55-OH	11	62	8		14	1.50·10 <sup>9</sup>	188	1.05
PDVB55-2	35		27	28				
PDVB55-BA	24	30	19		8	8.70·10 <sup>8</sup>	110	0.61
PDVB80-1	39		30	50				
PDVB80-OH	26	34	20		10	1.53·10 <sup>9</sup>	213	0.77
PDVB80-2	43		33	47				
PDVB80-BA	32	26	25		9	1.28·10 <sup>9</sup>	179	0.65

<sup>a</sup> *AS* (a.u.) are the active sites quantified with respect to the monomer units on the same arbitrary scale for all samples, via <sup>13</sup>C-CP MAS NMR spectroscopy.

<sup>b</sup> *ASAF* (%) are the active sites accessible for functionalization, quantified on an absolute scale by comparison of *AS* (a.u.) of the functionalized microspheres and of the corresponding core ones.

<sup>c</sup> *AS* (%) are the active sites quantified with respect to the monomer units on an absolute scale, obtained from *AS* (a.u.) via the same correction factor for all samples.

<sup>d</sup> *CL* (%) is the degree of crosslinking calculated on the corresponding core microsphere.

<sup>e</sup> *F*<sub>mon</sub> (%) is the degree of functionalization quantified in percents of the monomer units.

<sup>f</sup> *F*<sub>part</sub> (groups particle<sup>-1</sup>) is the number of active groups per particle.

<sup>g</sup> *F*<sub>surf</sub> (groups nm<sup>-1</sup>) is the number of active groups per nm<sup>2</sup>.

<sup>h</sup> *LC* (loading capacity) is the moles of active groups per gram of particle.

Equation (1) was used to determine the absolute percentages of residual vinyl groups in PDVB80: it was found that 30% of the monomer units contain residual vinyl groups. The percentage of active

sites of PDVB80 on the arbitrary scale was found to be 39%. Thus, a correcting factor of  $30/39=0.77$  must be applied to percentages of vinyl groups determined from  $^{13}\text{C}$  CP-MAS to convert them into actual percentages of vinyl groups, using equation (3):

$$AS (\%) = AS (\text{a.u.}) \cdot \frac{AS_{\text{PDVB80}} (\%) }{AS_{\text{PDVB80}} (\text{a.u.})} = AS (\text{a.u.}) \cdot 0.77 \quad (3)$$

The corrected values are given in Table 1 for all samples. Note that the active sites concentration measured by  $^{13}\text{C}$  CP-MAS is overestimated. This observed overestimation of the signal intensity for the vinyl methylene carbons with respect to that of the non-substituted aromatic carbons is attributed to the higher number of directly bound  $^1\text{H}$  nuclei (two versus one) leading to a more efficient polarization transfer, whereas the relaxation of the bound  $^1\text{H}$  nuclear spins under the applied radio-frequency field ( $T_{1\rho}$ ) can be expected to be identical (see Supporting Information for detailed discussion).

Several conclusions can be drawn from the comparison of the samples in terms of active sites quantified with respect to the monomer units on the same arbitrary scale via  $^{13}\text{C}$ -CP MAS NMR spectroscopy (Table 1, first and second columns). Firstly, PDVB80 samples have a higher degree of active sites  $AS$  (e.g. 41 a.u.) than PDVB55 ones (e.g. 32 a.u.). However, PDVB80 samples have proportionally less active sites accessible for functionalization  $ASAF$  (%) than PDVB55 ones. Both findings can be rationalized as follows. PDVB80 microspheres are synthesized from a monomer mixture with a higher proportion of difunctional monomer than PDVB55 ones, therefore they are expected to be more crosslinked, and consequently less swellable. This results in a higher number of active sites (vinyl groups) being trapped inside the microspheres, which are therefore not accessible for functionalization. Secondly, for both PDVB80 and PDVB55 systems, more active sites are accessible for functionalization ( $ASAF$  (%)) in the case of hydroxylation than in the case of grafting with *n*-butyl acrylate, BA. Such an observation is in agreement with the larger reagent size in the case of BA. Note that during the hydroxylation of sample PDVB80-OH, a side reaction leading to the hydrogenation of the vinyl group<sup>42</sup> leads to a signal increase in the pending ethyl groups observed at 16 and 30 ppm. Both hydroxylation

and hydrogenation of the vinyl group lead to the disappearance of this signal, thus in both cases the active site is quantified as being functionalized.

The quantification of active sites with respect to the monomer units on an absolute scale provides additional information (Table 1, third column). First, the core PDVB55 and PDVB80 microspheres have approximately 25 and 32% residual vinyl groups per monomer unit, while the initial monomer mixture contained 55 and 80% of difunctional monomer, respectively. Thus a significant fraction of the difunctional monomers have reacted only once (assuming there is no bias towards mono- or difunctional monomer the first time its reacts). This observation is consistent with an earlier report of significant amounts of residual vinyl groups in poly(styrene-*co*-divinyl benzene) networks, as soon as more than 10% divinyl benzene was used for the synthesis.<sup>17</sup> The resulting microspheres are highly crosslinked. The degree of crosslinking, defined as the proportion of monomer units which have reacted twice in the final polymer, may be calculated as follows:

$$CL (\%) = DM (\%) - AS (\%) \quad (4)$$

where  $DM (\%)$  is the proportion of difunctional monomer in the initial monomer mixture (55% for PDVB55 and 80% for PDVB80, respectively). Note that this formula holds only for the core microspheres before functionalization, and assumes that there is no bias towards mono- or difunctional monomer the first time a monomer unit reacts. The degree of crosslinking of the microspheres is high: approximately 30% for PDVB55 and approximately 50% for PDVB80 (Table 1, fourth column), which is much higher than the usual 2 to 10% observed in the more common poly(styrene-*co*-divinyl benzene) systems (e.g. Merrifield resins). The higher degree of crosslinking results in a lower swellability of PDVB80 compared to PDVB55 microspheres.

The extent of the functionalization may be quantified in different ways: with respect to the monomer units, to the number of groups per particle, to the nominal particle surface area and even as the loading capacity of the particles. The number of functional groups is easily calculated in percents of the monomer units as follows:

$$F_{\text{mon}} (\%) = \left( AS_{\text{core}} (\%) - AS_{\text{hydroxylated}} (\%) \right) \quad (5)$$

Hydroxylated microspheres have a higher number of functional groups per monomer unit,  $F_{\text{mon}}$ , than PBA-grafted ones, as was expected from the smaller reagent size. Interestingly, PDVB55 and PDVB80 microspheres exhibit a slightly different number of hydroxyl groups per monomer unit, but the same number of PBA grafts per monomer unit within experimental error.

The number of functional groups per particle may be calculated according to Equation 6:

$$F_{\text{part}} = \frac{F_{\text{mon}}(\%) \cdot n}{100} = \frac{(AS_{\text{core}}(\%) - AS_{\text{hydroxylated}}(\%))}{100} \cdot \frac{\pi \cdot d^3 \cdot \rho \cdot N}{6 \cdot M} \quad (6)$$

where  $n$  is the number of monomer units per particle,  $d$  is the particle diameter,  $\rho$  is the density of the PDVB microspheres (1.82 g·cm<sup>-3</sup> and 1.12 g·cm<sup>-3</sup> for PDVB80 and PDVB55 microspheres respectively),  $N$  is the Avogadro's number and  $M$  is the molar mass of the divinyl benzene monomer unit (130.19 g·mol<sup>-1</sup>). PDVB55 microspheres contain  $8.70 \cdot 10^8$  and PDVB80 microspheres contain  $1.28 \cdot 10^9$  active groups (e.g. vinyl groups) per particle that are accessible for grafting with BA.

The number of functional groups can also be expressed as number of functional groups per nominal surface area (groups per nm<sup>2</sup>). The calculation of the number of functional groups per surface area in the current study is based on the nominal surface area of a single microsphere, which does not take into account that the microsphere has a porous surface and the available surface area is clearly significantly larger than that nominally calculated. However, it is very difficult to obtain a suitable value for the accessible surface area, as this area is dependent on the type of molecule that is grafted as discussed earlier. The number of functional groups per nominal surface area (groups per nm<sup>2</sup>) may be calculated according to Equation 7:

$$F_{\text{surf}} = \frac{F_{\text{mon}}(\%) \cdot n}{100 \cdot SA} = \frac{(AS_{\text{core}}(\%) - AS_{\text{hydroxylated}}(\%))}{100} \cdot \frac{d \cdot \rho \cdot N}{6 \cdot M} \quad (7)$$

where  $SA$  is the nominal surface area of one microsphere. Derived from Equation 7, PDVB55 microspheres contain 110 and PDVB80 microspheres contain 179 active groups (e.g. vinyl groups) per nominal surface area, i.e. nm<sup>2</sup>, that are accessible for grafting with BA. Inspection of the ratio of the degree of crosslinking of the two types of particles ( $30/50 = 0.6$ ) and comparison with the ratio of the number of functional groups per nominal surface area of the two types of particles ( $110/179 = 0.61$ ) 20

demonstrates that the number of accessible active groups is directly linked with the degree of crosslinking.

In addition, the loading capacity  $LC$  (in  $\text{mmol}\cdot\text{g}^{-1}$ ) of the microspheres may be calculated according to Equation 8:

$$LC = \frac{6000 \cdot F_{\text{part}}}{\pi \cdot \rho \cdot N \cdot d^3} \quad (8)$$

The PDVB55-BA and PDVB80-BA microspheres have a loading capacity of 0.61 and 0.65  $\text{mmol}\cdot\text{g}^{-1}$ , respectively. These loading capacities are similar to the loading capacities found for Merrifield resins,<sup>43</sup> e.g. Merrifield resins of mesh size 100-200 (which corresponds to a particle diameter of 74 to 149  $\mu\text{m}$ ) have loading capacities from 1.5 to 4.5  $\text{mmol}\cdot\text{g}^{-1}$ .

## Conclusions

The potential of solid-state NMR spectroscopy to characterize surface functionalization in highly crosslinked microspheres is demonstrated. For the first time, residual vinyl groups were quantified in poly(divinyl benzene) microspheres in percents of the monomer units through solid-state NMR spectroscopy.  $^{13}\text{C}$  CP-MAS NMR spectroscopy allows the comparison of samples on the same arbitrary scale in a short measuring time. This scale was calibrated by one longer, absolute quantification of vinyl groups using  $^{13}\text{C}$  SPE-MAS NMR spectroscopy. Solid-state NMR spectroscopy detects all vinyl groups present in the sample, not distinguishing if they are located inside or at the surface of the particle. A comparison of core microspheres with the corresponding hydroxylated ones yields the proportion of the vinyl groups available for chemical functionalization. The proportion of the reacted vinyl groups is quantified by comparison of poly(*n*-butyl acrylate)-grafted microspheres with the corresponding core ones. It was found that not all vinyl groups available for functionalization were actually functionalized via grafting of BA. The degree of crosslinking was calculated to be 30% and 50% for PDVB55 and PDVB80 microspheres, respectively. The number of active groups per nominal surface area was 110

and 179 groups per nm<sup>-2</sup> for PDVB55 and PDVB80 microspheres, respectively. The loading capacities of the microspheres are similar to ones found in Merrifield resins of comparable sizes.

**Acknowledgements.** Funding from the *Max Planck Society* as well as the *Karlsruhe Institute of Technology* (KIT) is gratefully acknowledged. L.N., L.B. and C.B.-K. thank Dr. James Hook (NMR Facility, Analytical Centre, The University of New South Wales, Sydney, Australia) for fruitful discussions. In addition, M.G. and R.G. thank Prof. H. W. Spiess for continued support and his interest in the current work.

**Supporting information available:** full <sup>13</sup>C chemical shift assignment, <sup>1</sup>H and <sup>13</sup>C solid-state NMR spectra. This information is available free of charge via the Internet at <http://pubs.acs.org/>.

## References

1. Barner, L. *Adv. Mater.* **2009**, *21*, 2547-2553.
2. Kawaguchi, H. *Prog. Polym. Sci.* **2000**, *25*, 1171-1210.
3. Li, K.; Stoever, H. D. H. *J. Polym. Sci. A Polym. Chem.* **1993**, *31*, 3257-3263.
4. Barner, L. *Aust. J. Chem.* **2003**, *56*, 1091-1091.
5. Barner, L.; Li, C.; Hao, X. J.; Stenzel, M. H.; Barner-Kowollik, C.; Davis, T. P. *J. Polym. Sci. A Polym. Chem.* **2004**, *42*, 5067-5076.
6. Joso, R.; Stenzel, M. H.; Davis, T. P.; Barner-Kowollik, C.; Barner, L. *Aust. J. Chem.* **2005**, *58*, 468-471.
7. Lime, F.; Irgum, K. *J. Polym. Sci. A Polym. Chem.* **2009**, *47*, 1259-1265.
8. Zheng, G. D.; Stoever, H. D. H. *Macromolecules* **2002**, *35*, 6828-6834.
9. Joso, R.; Reinicke, S.; Walther, A.; Schmalz, H.; Mueller, A. H. E.; Barner, L. *Macromol. Rapid Commun.* **2009**, *30*, 1009-1014.
10. Goldmann, A. S.; Walther, A.; Nebhani, L.; Joso, R.; Ernst, D.; Loos, K.; Barner-Kowollik, C.; Barner, L.; Mueller, A. H. E. *Macromolecules* **2009**, *42*, 3707-3714.
11. Nebhani, L.; Barner-Kowollik, C. *Adv. Mater.* **2009**, *21*, 3442-3468.
12. Nebhani, L.; Schmiedl, D.; Barner, L.; Barner-Kowollik, C. *Adv. Func. Mater.* **2010**, submitted.
13. Nebhani, L.; Sinnwell, S.; Inglis, A. J.; Stenzel, M. H.; Barner-Kowollik, C.; Barner, L. *Macromol. Rapid Commun.* **2008**, *29*, 1431-1437.
14. Downey, J. S.; Frank, R. S.; Li, W. H.; Stoever, H. D. H. *Macromolecules* **1999**, *32*, 2838-2844.
15. Stoever, H. D. H.; Frechet, J. M. J. *Macromolecules* **1989**, *22*, 1574-1576.
16. Stoever, H. D. H.; Frechet, J. M. J. *Macromolecules* **1991**, *24*, 883-888.
17. Periyasamy, M.; Ford, W. T.; McEnroe, F. J. *J. Polym. Sci. A Polym. Chem.* **1989**, *27*, 2357-2366.
18. Ford, W. T.; Periyasamy, M.; Mohanraj, S.; McEnroe, F. J. *J. Polym. Sci. A Polym. Chem.* **1989**, *27*, 2345-2355.
19. Ford, W. T.; Mohanraj, S.; Hall, H.; O'Donnell, D. J. *J. Magn. Res.* **1985**, *65*, 156-158.
20. Schmidt-Rohr, K.; Spiess, H. W., *Multidimensional solid-state NMR and polymers*. 1st ed.; Academic Press Ltd: San Diego, USA, 1994.
21. Gaborieau, M.; Graf, R.; Spiess, H. W. *Solid State Nucl. Magn. Reson.* **2005**, *28*, 160-172.
22. Gaborieau, M.; Graf, R.; Kahle, S.; Pakula, T.; Spiess, H. W. *Macromolecules* **2007**, *40*, 6249-6256.
23. Gaborieau, M.; Graf, R.; Spiess, H. W. *Macromol. Chem. Phys.* **2008**, *209*, 2078-2086.
24. Castignolles, P.; Graf, R.; Parkinson, M.; Wilhelm, M.; Gaborieau, M. *Polymer* **2009**, *50*, 2373-2383.
25. Gaborieau, M.; DeBruyn, H.; Mange, S.; Castignolles, P.; Brockmeyer, A.; Gilbert, R. G. *J. Polym. Sci. A Polym. Chem.* **2009**, *47*, 1836-1852.
26. Hartmann, S. R.; Hahn, E. L. *Phys. Rev.* **1962**, *128*, 2042-2053.
27. Schaefer, J.; Stejskal, E. O.; Buchdahl, R. *Macromolecules* **1977**, *10*, 384-405.
28. Metz, G.; Ziliox, M.; Smith, S. O. *Solid State Nucl. Magn. Reson.* **1996**, *7*, 155-160.
29. Hou, G. J.; Deng, F.; Ye, C. H.; Ding, S. W. *J. Chem. Phys.* **2006**, *124*, 234512.
30. Fu, R. Q.; Hu, J.; Cross, T. A. *J. Magn. Reson.* **2004**, *168*, 8-17.
31. Shu, J.; Chen, Q.; Zhang, S. M. *Chem. Phys. Lett.* **2008**, *462*, 125-128.
32. Pollard, M.; Klimke, K.; Graf, R.; Spiess, H. W.; Wilhelm, M.; Sperber, O.; Piel, C.; Kaminsky, W. *Macromolecules* **2004**, *37*, 813-825.
33. Perrier, S.; Barner-Kowollik, C.; Quinn, J. F.; Vana, P.; Davis, T. P. *Macromolecules* **2002**, *35*, 8300-8306.
34. Bai, F.; Yang, X. L.; Huang, W. Q. *Macromolecules* **2004**, *37*, 9746-9752.
35. Beuermann, S.; Paquet, D. A.; McMinn, J. H.; Hutchinson, R. A. *Macromolecules* **1996**, *29*, 4206-4215.
36. Rudin, A.; Hoegy, H. L. W. *J. Polym. Sci. A1 Polym. Chem.* **1972**, *10*, 217-235.



37. Gaborieau, M.; Gilbert, R. G.; Gray-Weale, A.; Hernandez, J. M.; Castignolles, P. *Macromol. Theory Simul.* **2007**, *16*, 13-28.
38. Gaborieau, M.; Nicolas, J.; Save, M.; Charleux, B.; Vairon, J. P.; Gilbert, R. G.; Castignolles, P. *J. Chromatogr. A* **2008**, *1190*, 215-223.
39. Castignolles, P. *Macromol. Rapid Commun.* **2009**, *30*, 1995-2001.
40. NMR spectra database of polymers, [http://polymer.nims.go.jp/NMR/top\\_eng.html](http://polymer.nims.go.jp/NMR/top_eng.html).
41. Spectral database for organic compounds SDBS, [http://www.aist.go.jp/RIODB/SDBS/cgi-bin/cre\\_index.cgi](http://www.aist.go.jp/RIODB/SDBS/cgi-bin/cre_index.cgi).
42. Westcott, S. A.; Blom, H. P.; Marder, T. B.; Baker, R. T.; Calabrese, J. C. *Inorg. Chem.* **1993**, *32*, 2175-2182.
43. Sigma-Aldrich catalog, <http://www.sigmaaldrich.com/>.

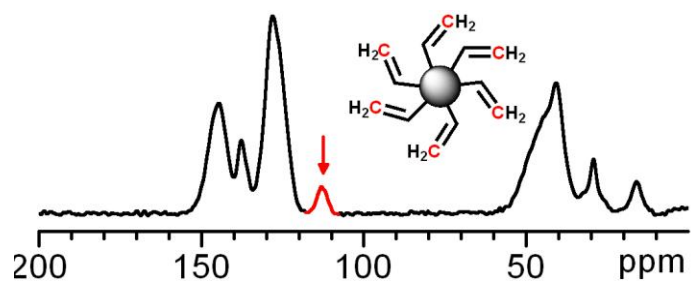
**For Table of Contents use only**

Accessing Quantitative Degrees of Functionalization on Solid Substrates via Solid State NMR

Spectroscopy

Marianne Gaborieau, Leena Nebhani, Robert Graf, Leonie Barner, Christopher Barner-

Kowollik



Supporting Information for

# Accessing Quantitative Degrees of Functionalization on Solid Substrates via Solid State NMR Spectroscopy

*Marianne Gaborieau,\* Leena Nebhani, Robert Graf, Leonie Barner\*,*

*Christopher Barner-Kowollik\**

<sup>1</sup>Max Planck Institute for Polymer Research, Ackermannweg 10, 55128 Mainz, Germany,  
m.gaborieau@uws.edu.au, graf@mpip-mainz.mpg.de

<sup>2</sup>Preparative Macromolecular Chemistry, Institut für Technische Chemie und Polymerchemie,  
Karlsruhe Institute of Technologie (KIT), Engesserstrasse 18, 76128 Karlsruhe, Germany,  
leena.nebhani@kit.edu, christopher.barner-kowollik@kit.edu

<sup>3</sup>Fraunhofer Institut für Chemische Technologie, Joseph-von-Fraunhofer-Strasse 7, 76327  
Pfinztal (Berghausen), Germany, leonie.barner@ict.fraunhofer.de.

**Figure S1:  $^1\text{H}$  MAS spectrum of sample PDVB80 with residual monomer**

The weak narrow signals were originally observed at 5.2, 6.2 and 6.7 ppm for sample PDVB80 originate in vinyl groups. They disappeared upon repeated washing of the sample with toluene. They were thus assigned to residual monomers rather than active sites (residual vinyl groups on the polymer chains). Care was taken to ensure that all core PDVB microspheres used for the present work had been washed appropriately to remove any residual monomer, before functionalization or NMR measurement. This is particularly important since the signal of vinyl groups from residual monomer would overlap with those from the polymer chains, inducing an error in the active sites quantified by  $^{13}\text{C}$  NMR.

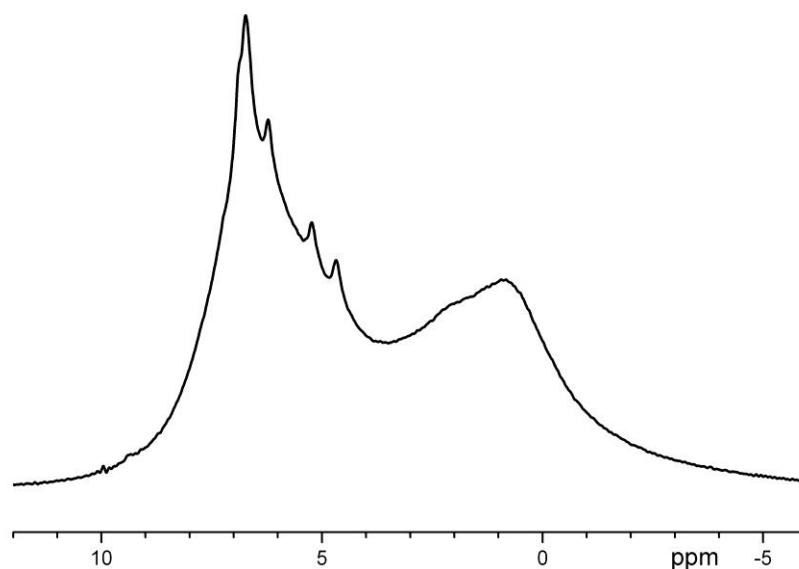


**Table S-1: Full  $^{13}\text{C}$  chemical shifts assignment**

Complete  $^{13}\text{C}$  chemical shifts assignment for  $^{13}\text{C}$  NMR spectra of core, hydroxylated and PBA-grafted poly(divinyl benzene) microspheres (chemical formulae given in Scheme 1). Letters refer to Scheme 1.

<i>Group</i>	<i>Chemical shift / ppm</i>	<i>Assignment</i>
L	13	CH <sub>3</sub> of side chain of PBA
G	16	CH <sub>3</sub> of ethyl on aromatic ring
K	20	CH <sub>2</sub> of side chain of PBA in $\alpha$ of CH <sub>3</sub>
J	29, 31	CH <sub>2</sub> of side chain of PBA adjacent to O-CH <sub>2</sub> -
F	30	CH <sub>2</sub> from ethyl on aromatic ring
E	41-50	CH backbone PDVB and PBA CH <sub>2</sub> backbone PDVB and PBA
I	64	CH <sub>2</sub> of ethyl-OH in $\alpha$ of aromatic ring (if OH in $\beta$ of ring) O-CH <sub>2</sub> of side chain of PBA
D	113	C=C (C not adjacent to aromatic ring)
C	128	benzene ring (not substituted) of PDVB or RAFT group
B	138	C=C (C adjacent to aromatic ring)
A	146	aromatic ring (adjacent to C=C, or to ethyl-OH if OH in $\alpha$ of ring) aromatic ring (adjacent to ethyl or backbone, or to ethyl-OH if OH in $\alpha$ of ring, or to C=S in RAFT group)
H	166	C=O of PBA

It was checked that the presence of 2 substituents in meta or para on the aromatic ring did not change the chemical shift of aromatic C to the point that they would come out in another massif observed by solid-state NMR.

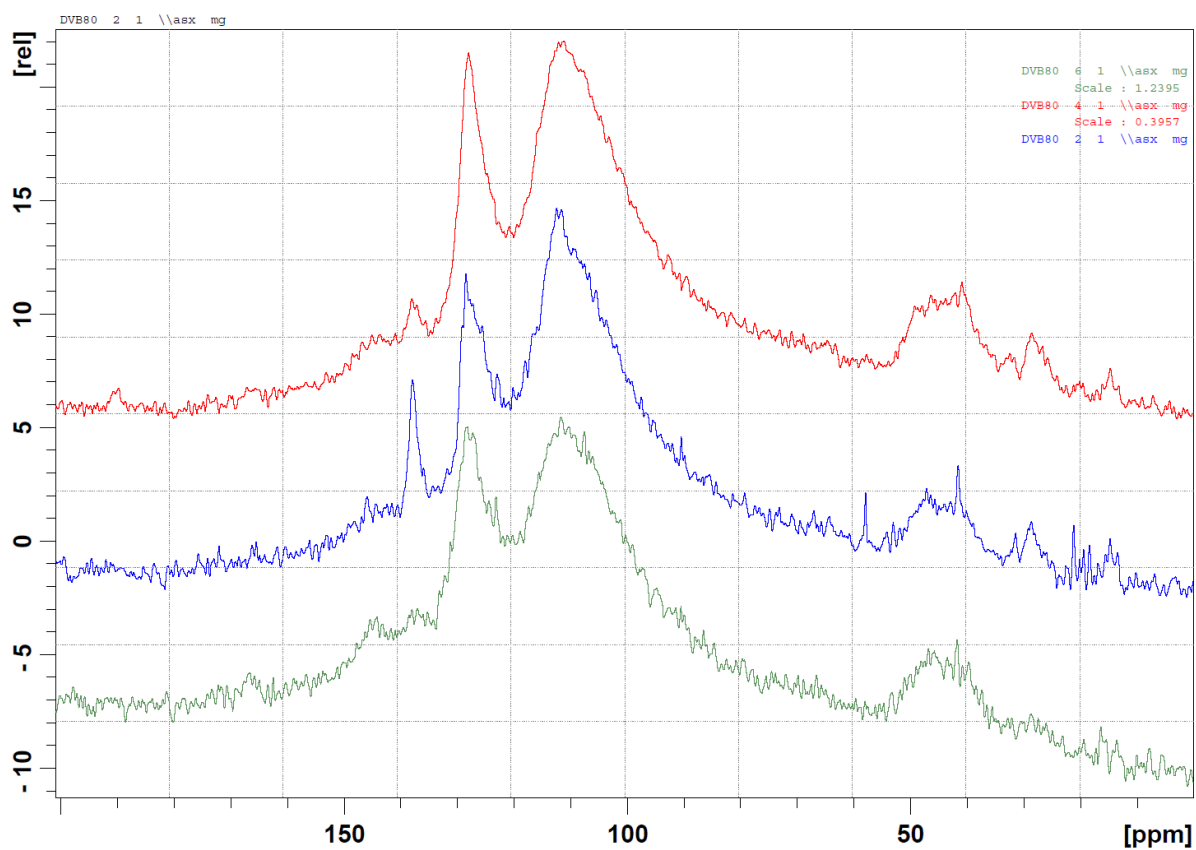
Note: the following signals were below the detection limit:

- CH<sub>3</sub> of ethyl-OH (if OH in  $\alpha$  of ring), expected at ca. 25 ppm
- CH<sub>2</sub> of ethyl-OH in  $\beta$  of aromatic ring (if OH in  $\beta$  of ring), expected at ca. 63 ppm
- CH from ethyl-OH (if OH in  $\alpha$  of ring), expected at ca. 70 ppm
- C=S of RAFT group, expected at ca. 225 ppm

**Figure S2: No influence of temperature on broad underlying signal**

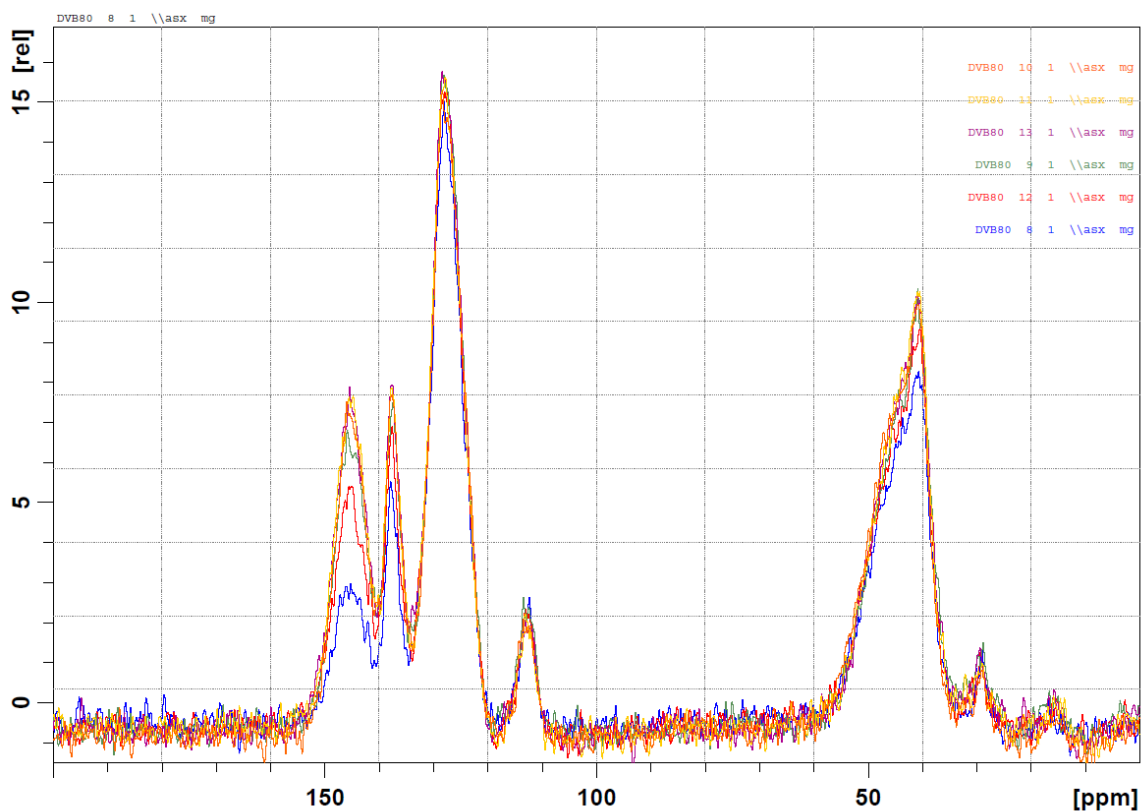
Variable-temperature experiments revealed that the broad underlying signal in the aromatic region does not originate in highly-crosslinked samples parts, but is actually a background signal from the rotor caps and the probes.

Experimental conditions: Bruker Avance 500, 4 mm MAS probe, ZrO<sub>2</sub> rotor with BN cap, 10 kHz MAS, <sup>13</sup>C SPE-MAS, 4 μs 90° pulse, 10 s repetition delay, no temperature calibration thus approximate temperatures; at 150 °C with NS = 1 360 in 3 h 50; at 200 °C with NS = 4 038 in 11 h 20; at 100 °C with NS = 1 024 in 2 h 50.



**Figure S3: Influence of contact time on signal intensities in  $^{13}\text{C}$  CP-MAS spectra**

Experimental conditions: Bruker Avance 500, 2.5 mm MAS probe, room temperature, 18 kHz MAS,  $^{13}\text{C}$  CP-MAS,  $2.5\ \mu\text{s}$   $90^\circ$  pulse, 5 s repetition delay ; PDVB80 with 1 536 transients in 2 h 10 and contact times of  $250\ \mu\text{s}$ ,  $500\ \mu\text{s}$ , 1 ms, 1.5 ms , 2 ms and 3 ms; PDVB80BA with 1 256 transients in 1 h 46 and contact times of  $500\ \mu\text{s}$ , 1 ms, 2 ms, 3 ms; PDVB55 with 1 024 transients in 1 h 26 and contact times of  $250\ \mu\text{s}$ ,  $500\ \mu\text{s}$ , 1 ms, 2 ms, 2.5 ms, 3 ms; PDVB55BA with 1 536 transients in 2 h 10 and contact times of  $250\ \mu\text{s}$ ,  $500\ \mu\text{s}$ , 1 ms, 2 ms, 2.5 ms, 3 ms.



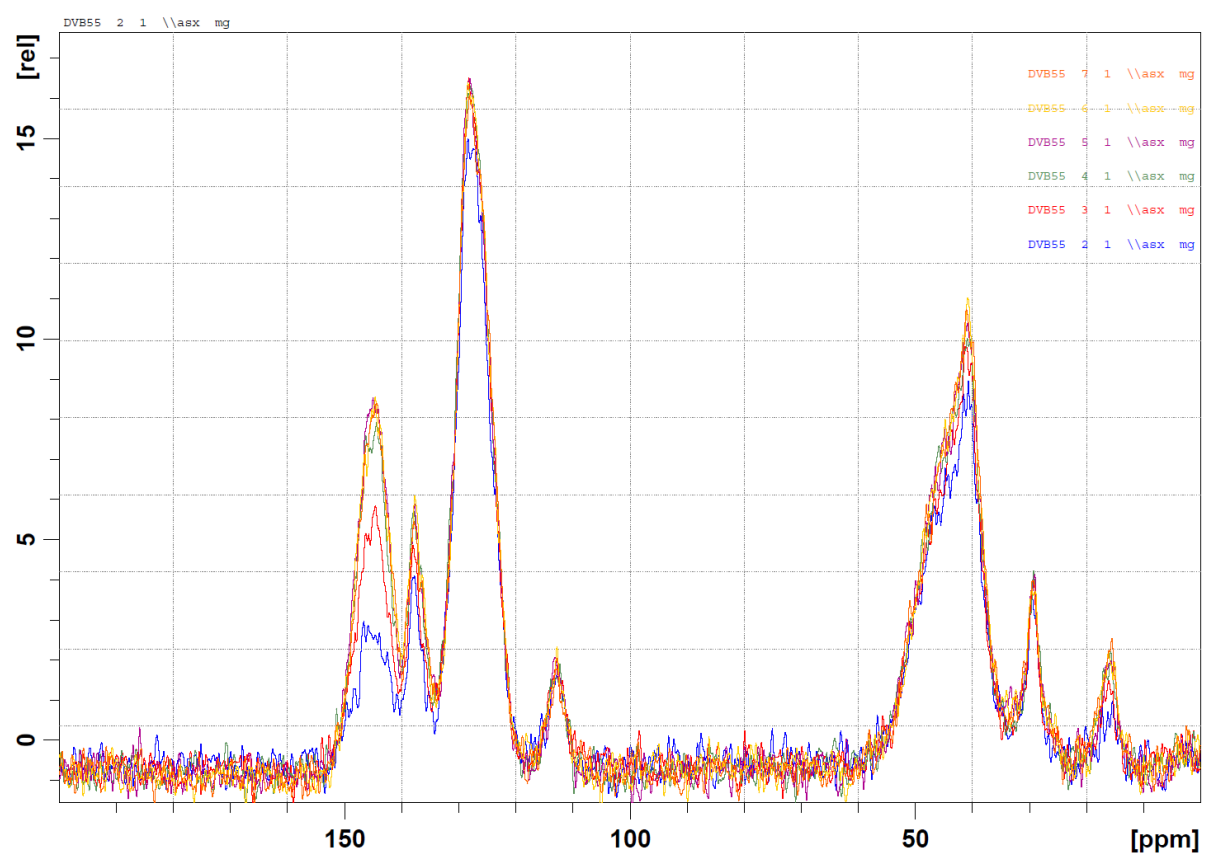
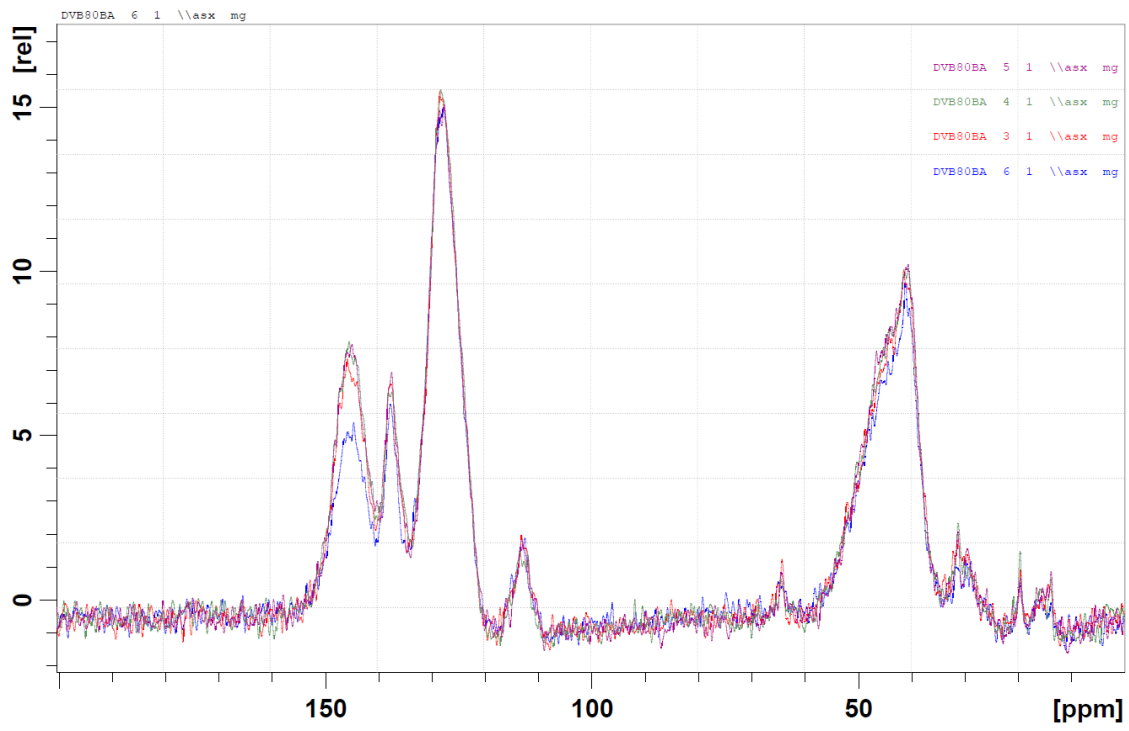
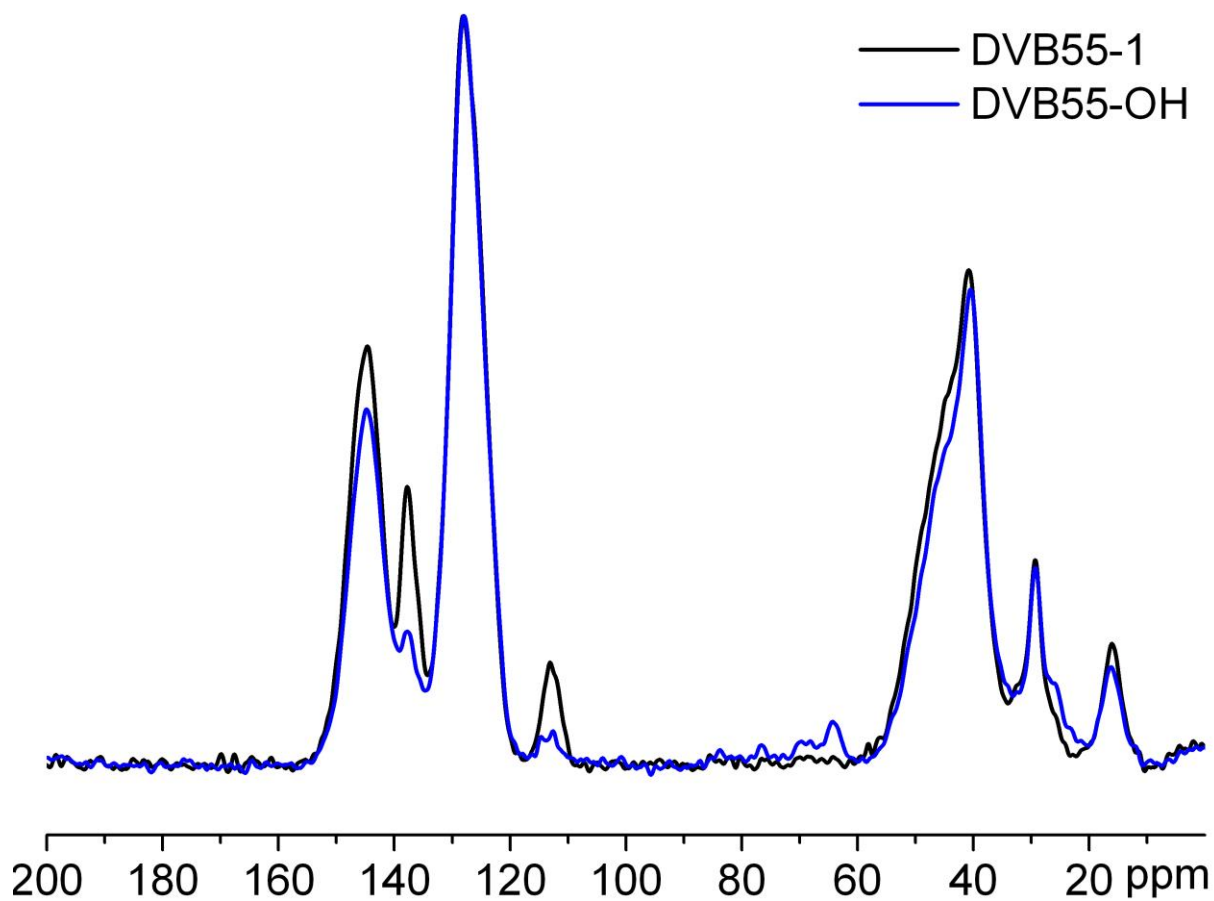


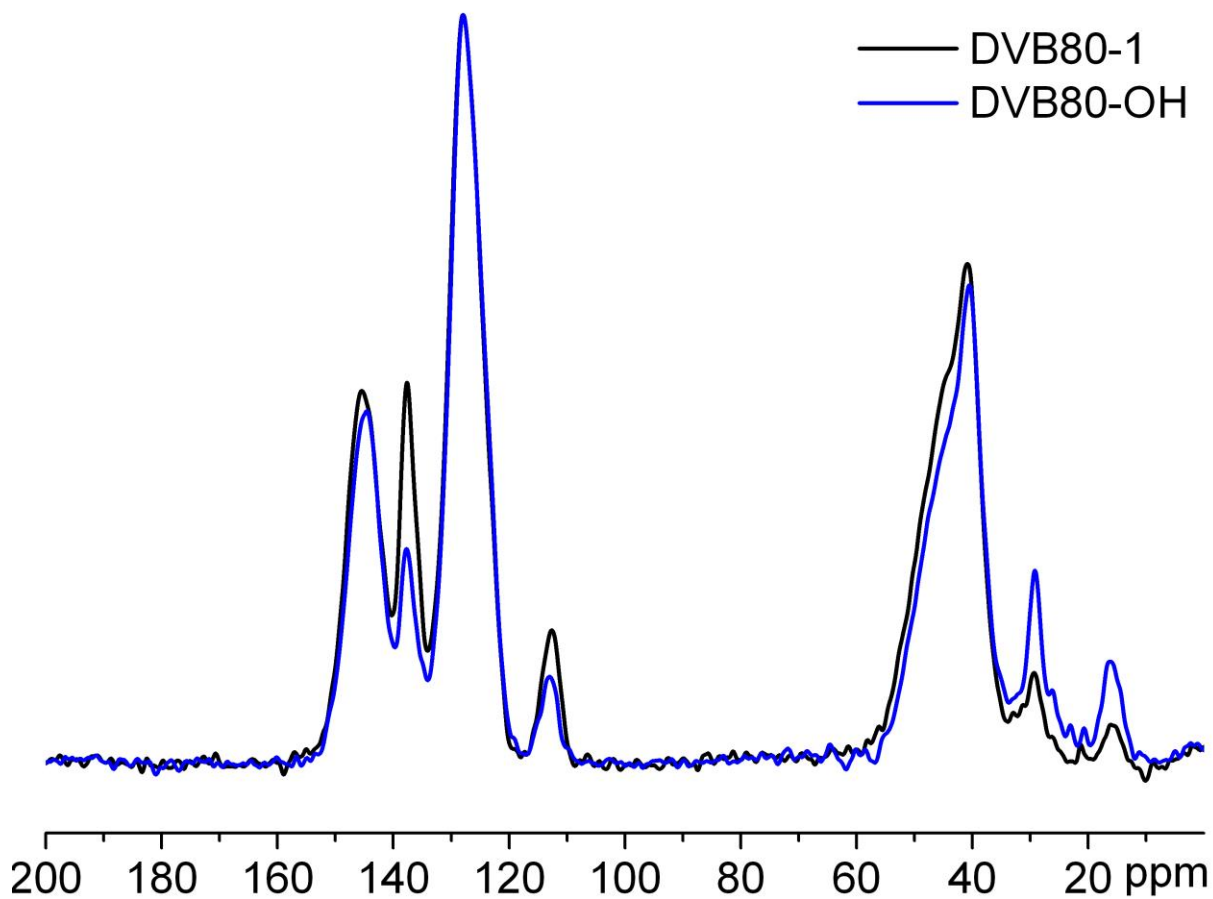
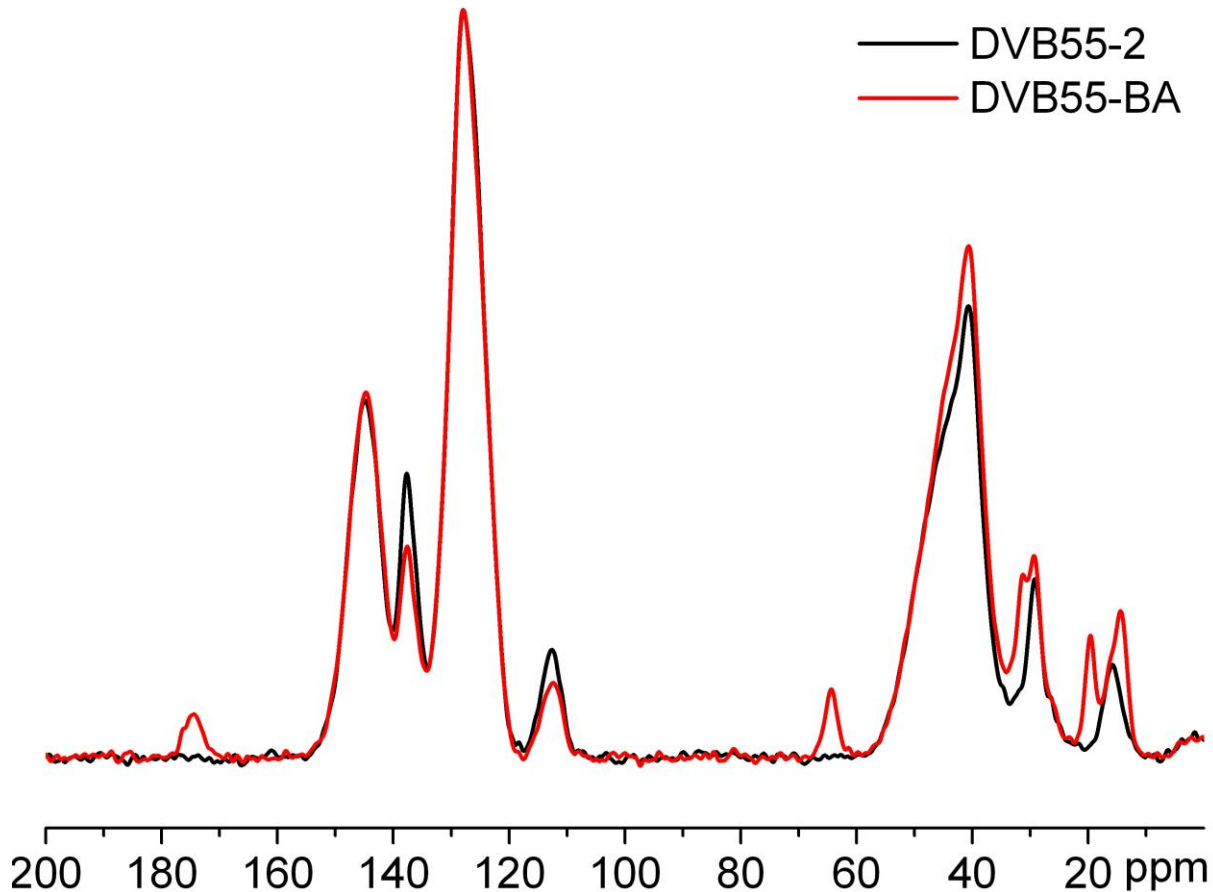




**Figure S4: Semi-quantitative  $^{13}\text{C}$  CP-MAS spectra**

Experimental conditions:  $^{13}\text{C}$  CP-MAS, semi-quantitative: Avance 500, 2.5 mm MAS probe, 18 kHz MAS,  $2.5\ \mu\text{s}$   $90^\circ$  pulse, 5 s repetition delay,  $T_{\text{cp}} = 2\text{ms}$ , NS = 5 632, expt = 7 h 54.





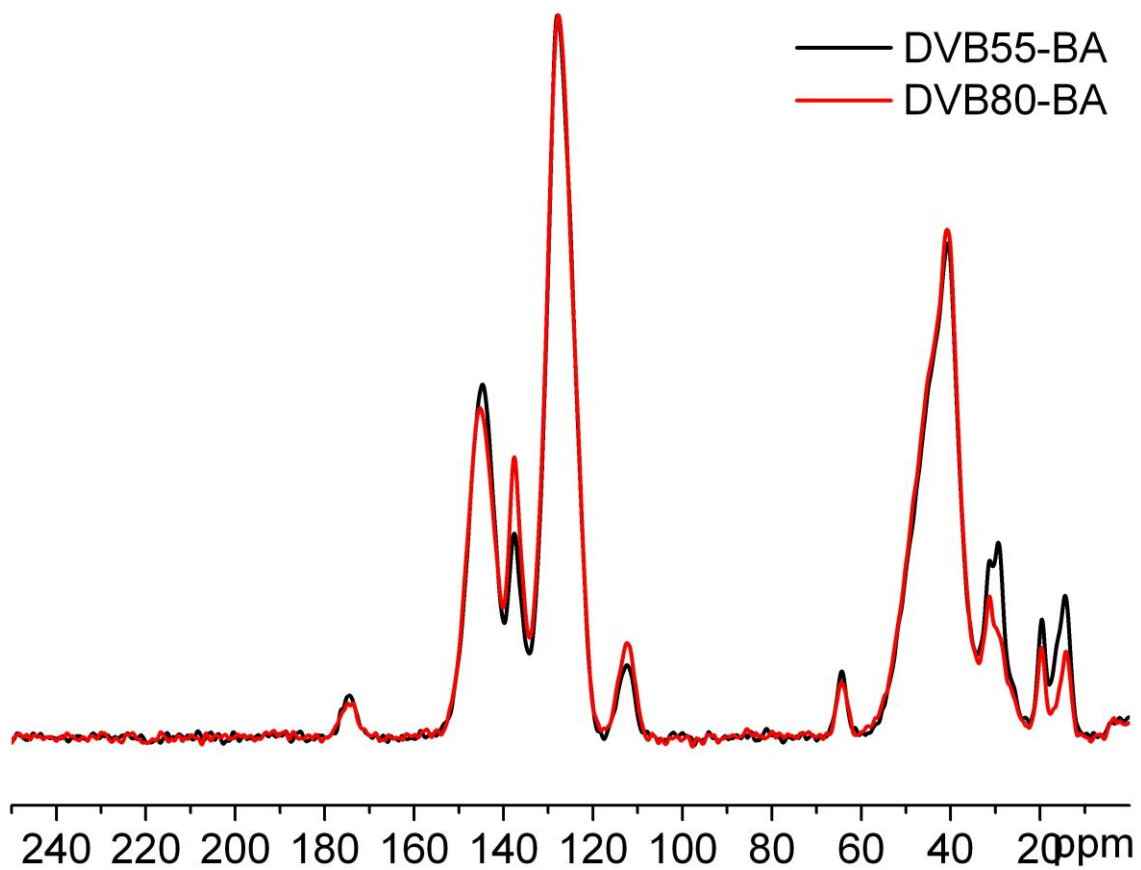
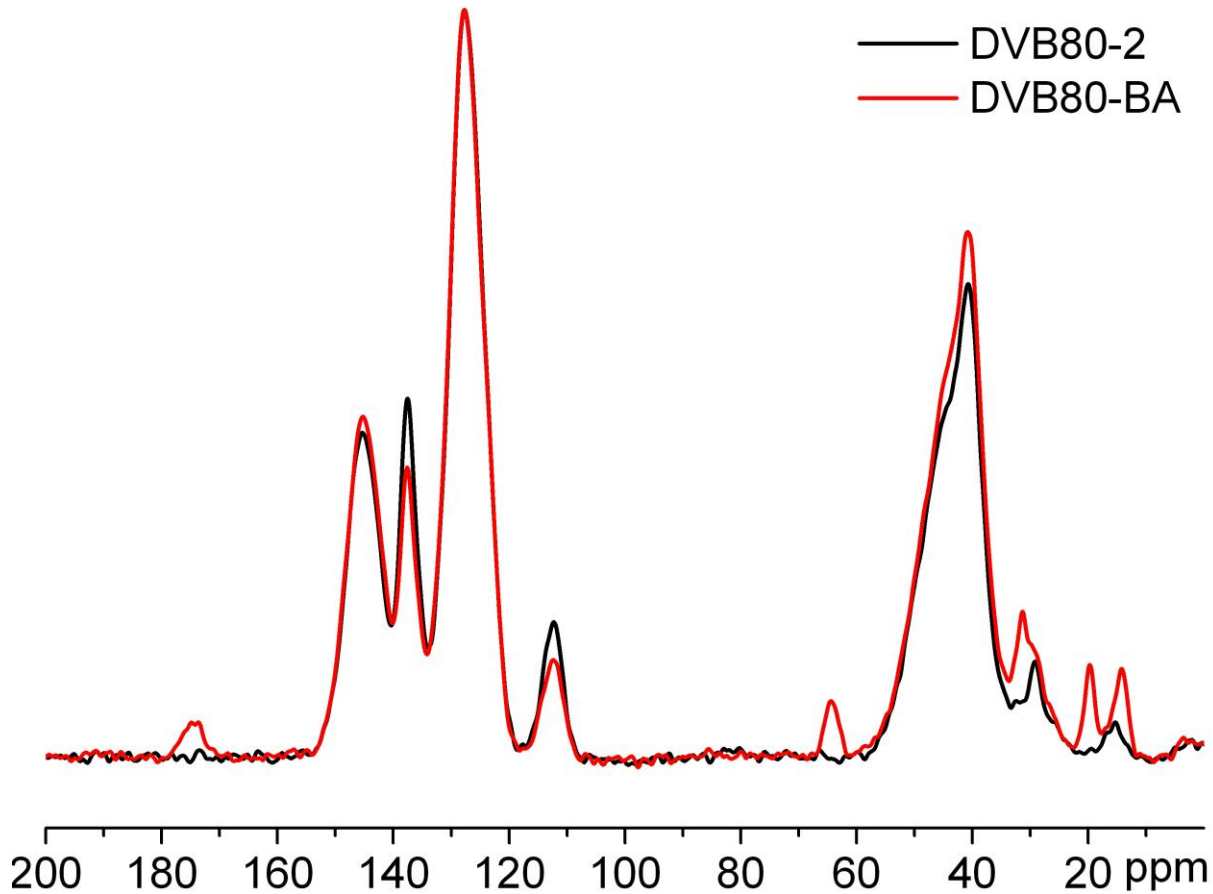
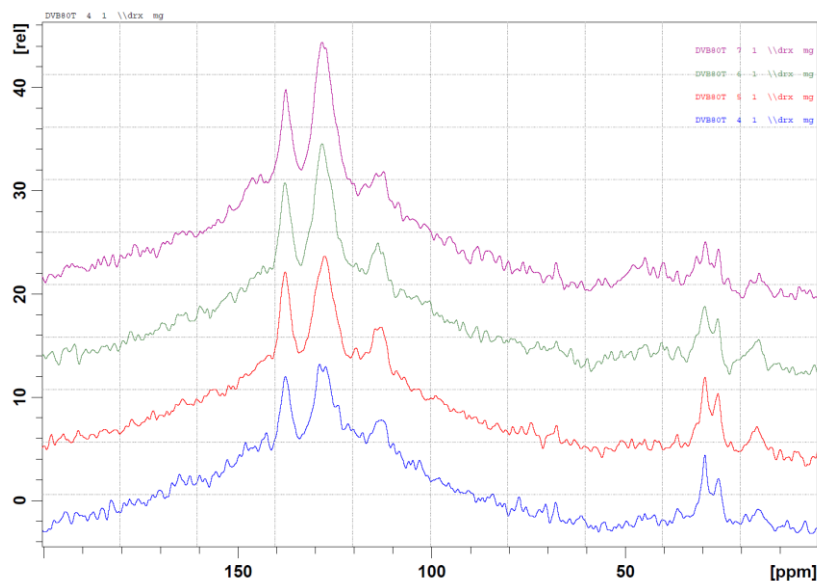
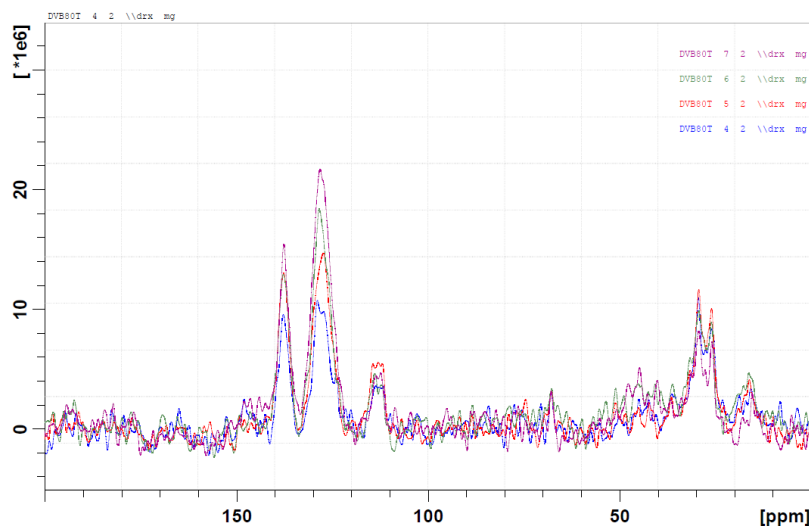


**Figure S5: Determining conditions for quantitative  $^{13}\text{C}$  SPE-MAS spectra**

Spectra recorded with relaxation delays ranging from 2 to 20 s. Due to limited sensitivity, no significant difference between spectra recorded with 10 and 20 s.



However, after the background signal was recorded on another day, the background subtraction was done, yielding the spectra below.



It is now obvious that there is a big difference in the signal C at ca 128 ppm between 10 and 20 s. Thus 10 s relaxation delay is not sufficient to record a quantitative  $^{13}\text{C}$  SPE-MAS spectrum of PDVB80. As it would be too time-consuming to test various longer relaxation delays, it was decided to directly use a very long relaxation delay (60 s) and record the  $^{13}\text{C}$  SPE-MAS spectra of PDVB80 and the background.

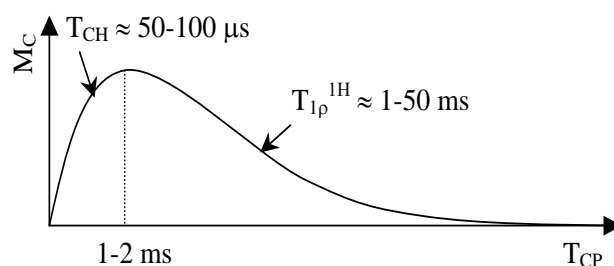
### *Discussion of the overestimation of AS by <sup>13</sup>C CP-MAS measurements*

The active sites concentration measured by <sup>13</sup>C CP-MAS is overestimated, meaning that the signal intensity for the vinyl methylene carbons is overestimated with respect to that of the non-substituted aromatic carbons.

The <sup>13</sup>C CP-MAS experiment is divided in three parts: first the flip of the hydrogen magnetization to the xy-plane, then the transfer of the magnetization between <sup>1</sup>H and <sup>13</sup>C nuclei in the xy-plane via cross-polarization during a time T<sub>CP</sub>, followed by the recording of the FID. During T<sub>CP</sub>, polarization transfer is possible via heteronuclear dipole-dipole interactions since the <sup>1</sup>H spins are locked with an rf field B<sub>1</sub><sup>1H</sup>, while the <sup>13</sup>C spins are irradiated with a different magnetic field B<sub>1</sub><sup>13C</sup> = 4·B<sub>1</sub><sup>1H</sup>, so that they finally have the same precession frequency  $\omega^C = \gamma^C \cdot B_1^C = \gamma^H \cdot B_1^H = \omega^H$  in the locking fields (so-called Hartmann-Hahn conditions). During T<sub>CP</sub>, both <sup>1</sup>H and <sup>13</sup>C loose magnetization (in the xy-plane) through T<sub>1ρ</sub> relaxation phenomena (corresponding to the relaxation under an applied radio-frequency field). Efficient magnetization transfer is possible only if the relaxation time constants T<sub>1ρ</sub> are higher than the time constant T<sub>CH</sub> of the magnetization transfer. As the cross-polarization and the T<sub>1ρ</sub> relaxation of the <sup>1</sup>H nuclei are the fastest phenomena, the intensity M<sub>C</sub>(t) of the <sup>13</sup>C nuclei magnetization over time approximately follows the equation:

$$M_C(t) = M_0 \cdot e^{-t/T_{1\rho}} \cdot (1 - e^{-t/T_{CH}})$$

where M<sub>0</sub> is the initial <sup>1</sup>H magnetization, T<sub>1ρ</sub> the longitudinal relaxation time of <sup>1</sup>H nuclei under Hartmann-Hahn conditions, and 1/T<sub>CH</sub> the magnetization transfer rate from <sup>1</sup>H to <sup>13</sup>C nuclei under Hartmann-Hahn conditions (ref Grimmer, A. R.; Bluemich, B.; Introduction to Solid-State NMR, In NMR Basic Principles and Progress, 1994; vol. 30, pp 1-62). The intensity of the magnetization of a <sup>13</sup>C nucleus as a function of the contact time T<sub>CP</sub> is sketched on the figure below (typical time constants are indicated):



From these two time constants,  $T_{CH}$  and  $T_{1\rho}$ , we expect  $T_{CH}$  to contribute predominantly to the observed overestimation of the signal intensity for the vinyl methylene carbons with respect to that of the non-substituted aromatic carbons. First,  $T_{1\rho}$  can be expected to be very similar for the vinyl proton sites and the aromatic protons, since the vinyl group is directly bound to the aromatic ring leading to a conjugation of the vinyl double bond and the aromatic ring, which excludes molecular motions with correlation times differing on a logarithmic scale needed to cause different  $T_{1\rho}$  relaxation times. The shorter  $T_{CH}$  of the vinyl group can be attributed to the fact that the vinyl methylene carbons are bound to two  $^1H$  nuclei each, while the non-substituted aromatic ones are bound to only one each. Moreover the shorter  $T_{CH}$  of the vinyl methylene group is supported by the experimental finding that the CP-MAS signal of this group build up fastest with short CP contact times, as shown in figure 3, whereas all other signals need longer CP contact times to achieve contact time independent relative intensities.